

A COMPARISON AMONG SOME LOCAL APPROXIMATION IN ONE-DIMENSIONAL PROFILE RECONSTRUCTION

J. A. K. Adopley and D. G. Dudley
Electromagnetics Laboratory
ECE, Building 104
The University of Arizona
Tucson, AZ 85721, USA

T. M. Habashy
Schlumberger-Doll Research
Old Quarry Road
Ridgefield, CT 06877-4108, USA

- 1. Introduction**
 - 2. Integral Equation of the Slab Problem**
 - 2.1 General Local Approximation
 - 2.2 First Approximation
 - 2.3 Second Approximation
 - 3. Numerical Results**
 - 4. Inversion Algorithm**
 - 4.1 Numerical Inversion Studies
 - 5. Conclusion**
- References**

1. INTRODUCTION

The task of electromagnetic profile inversion is extracting information about a material object from electromagnetic phenomena observed or measured outside the material medium. The intrinsic feature that sets these inversion problems apart from parameter estimation is that

the unknowns are usually functions of space and time (or frequency). The implication is that, in principle, the solution contains an infinite number of variables and hence the problem is as underdetermined as it possibly can be. In addition, inverse problems are well known to be nonunique. The nonuniqueness of electromagnetic inverse problems have been well documented in the literature [1–10] and will not be considered here. Rather, we shall investigate the effectiveness of the localized approximations as originally proposed by Habashy et al. [11], and extensions thereto. As a vehicle for study, we consider a one spatial dimension problem involving scattering from a lossy dielectric slab, herein referred to as *the slab problem*.

The one-dimensional integral equation that describes the functional relationship between observed (or measurable) electromagnetic phenomena outside of the one-dimensional slab and its constitutive electromagnetic parameters seems deceptively simple. The difficulty is embedded in the integrand of the integral equation. This integrand is the product of the unknown total internal electric fields, a Green's function, and the unknown contrast in complex conductivity (or permittivity). Additionally, the total internal electric field is functionally dependent on the slab complex conductivity profile. This renders the problem nonlinear. The starting point in obtaining a solution is finding an acceptable accurate approximation to the internal electric field. The first efforts in this direction were by Born [12] and Rytov [13]. The potentials and limitations of the two approximations have been reviewed extensively in the electromagnetic literature [14, 11, 16, 17]. Beyond the well known approximations of Born and Rytov, Habashy et al. [11] proposed a nonlinear localized approximation based on the recognition that the Green's function has a singularity (in multidimensional problems) when computing the total internal electric field at the source point. Hence for internal fields that are smoothly varying, the field at the source point can be approximated by the field at the observation point. This approximation allows the internal electric field to be explicitly determined from the Green's function and the complex conductivity contrast. As pointed out by Torres-Verdin and Habashy [18], the technique is more difficult to apply in one-dimensional problems where the Green's function singularity degenerates into a localized peak or maximum.

Herein, we modify the localized approximation by introducing two iterative techniques in order to partially circumvent the difficulties in

one-dimension. In the first technique we iterate the governing equation once before adopting the localized approximation in [11], while in the second case we apply the iteration once after the localized approximation. We also develop a generalization of the iterative techniques using the extended Born approximation.

The first part of this paper deals with the evaluation of the effectiveness of the localized approximation (and modifications) in improving and/or enhancing accurate simulation of the total internal electric field. The second part deals with the reconstruction of the slab conductivity profiles from noise contaminated synthetic data using the localized approximations and the modifications. We have adopted Occam's method [37, 20] in our inversion for its robustness and versatility. It is a least-squares method that produces the "smoothest" model based on minimizing the integral of the squares of the first or second derivative of the complex conductivity profile with respect to the slab axis. A generalization of the method has been proposed by Smith et al. [38].

In the next section, we present the formulation of the localized approximation with the two extensions. In addition, we extend the Trantenella approximation [19, 21] to include lossy profiles. (In their study Trantanella et al. [21] modified the Born approximation by including both a forward and a reflected wave approximation to the internal fields.)

In section 3, we perform numerical simulations for piecewise constant and linear complex conductivity profiles. These results are evaluated against exact solutions from transmission-line theory. We provide representative results from exhaustive numerical study on the influence of both displacement and conduction currents.

In section 4, we give a brief description and formalism of Occam's method with some reconstruction results performed on noisy synthetic data. In the last section we draw some conclusions from our work and point to the direction of future work.

2. INTEGRAL EQUATION OF THE SLAB PROBLEM

The geometry of the problem is as shown in Figure 1. The integral equation that describes the electric field is given by

$$E_y(z) = E_y^{in}(z) + \frac{k_b}{2j\epsilon_b} \int_0^d q(z')g(z, z')E_y(z')dz' \quad (1)$$

which is valid everywhere in space. Here the subscript b refers to the

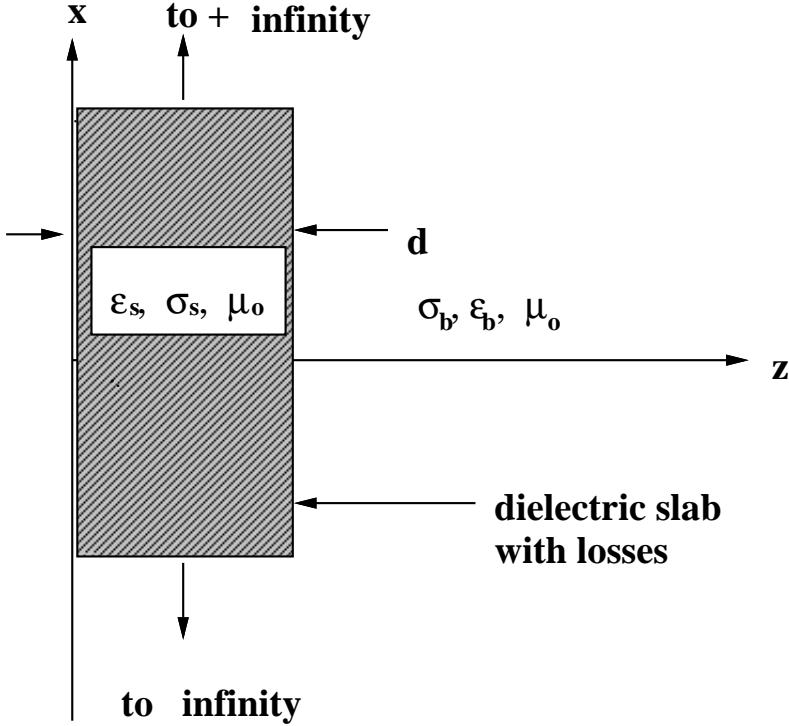


Figure 1. Dielectric slab with complex permittivity.

background medium and $q(z) = \epsilon_s(z) - \epsilon_b$ is the relative permittivity profile of the slab. All other quantities have their usual meanings. The Green's function $g(z, z')$ is defined for the 1-dimensional slab problem to be

$$g(z, z') = e^{-jk_b|z-z'|} \quad (2)$$

In the Habashy approximation [11], the field at the source point is approximated by the field at the observation point for observation points limited to within the scatterer. In this way we can rewrite the integral equation as

$$\begin{aligned} E_y(z) = & E_y^{in}(z) + \frac{k_b}{2j\epsilon_b} \int_0^d q(z')g(z, z')E_y(z)dz' \\ & + \frac{k_b}{2j\epsilon_b} \int_0^d q(z')g(z, z')[E_y(z') - E_y(z)]dz' \end{aligned} \quad (3)$$

and we obtain after some algebraic manipulation

$$E_y(z) = \Gamma(z) \left[E_y^{in}(z) + \frac{k_b}{2j\epsilon_b} \int_0^d q(z')g(z, z')[E_y(z') - E_y(z)]dz' \right] \quad (4)$$

where $\Gamma(z)$ is defined by

$$\Gamma(z) = \left[1 - \frac{k_b}{2j\epsilon_b} \int_0^d q(z')g(z, z')dz' \right]^{-1} \quad (5)$$

In the Habashy approximation, the internal electric field, $E_y(z)$ is given by

$$E_y(z) \approx \Gamma(z)E_y^{in}(z) \quad (6)$$

with error given by

$$\Gamma(z) \left[\frac{k_b}{2j\epsilon_b} \int_0^d q(z')g(z, z')[E_y(z') - E_y(z)]dz' \right] \quad (7)$$

In our attempt to extend the domain of validity of the above approximation, we employ two iterative techniques. In the first case which we call the Adopley approximation, we iterate the integral equation once before employing the localized approximation. In the second case which we call the Extended Habashy approximation, we iterate the localized approximation once. Specifically, the internal field in the Adopley approximation is written as

$$E_y(z') = E_y^{in}(z') + \frac{k_b}{2j\epsilon_b} \int_0^d q(\xi')g(z', \xi')E_y(\xi')d\xi' \quad (8)$$

When this is substituted back into the integral equation, we obtain

$$E_y(z) = E_y^{in}(z) + \frac{k_b}{2j\epsilon_b} \int_0^d q(z')g(z, z') [E_y^{in}(z') + \frac{k_b}{2j\epsilon_b} \int_0^d q(\xi')g(z', \xi')E_y(\xi')d\xi'] dz' \quad (9)$$

We incorporate the Habashy approximation by replacing $E_y(\xi')$ with $E_y(z)$ in the above equation to obtain

$$E_y(z) = E_y^{in}(z) + \frac{k_b}{2j\epsilon_b} \int_0^d q(z')g(z, z')E_y^{in}(z')dz' + E_y(z) \left(\frac{k_b}{2j\epsilon_b} \right)^2 \int_0^d dz' \int_0^d q(z')g(z, z')q(\xi')g(z', \xi')d\xi' \quad (10)$$

We then solve for $E_y(z)$ to get

$$E_y(z) = \left[E_y^{in}(z) + \frac{k_b}{2j\epsilon_b} \int_0^d q(z')g(z, z')E_y^{in}(z')dz' \right] \Gamma(z) \quad (11)$$

where $\Gamma(z)$ is given by

$$\Gamma(z) = \left[1 + \left(\frac{k_b}{2j\epsilon_b} \right)^2 \int_0^d dz' \int_0^d q(z')g(z, z')q(\xi')g(z', \xi')d\xi' \right]^{-1} \quad (12)$$

The error introduced is then given by

$$\Gamma(z) \left(\frac{k_b}{2j\epsilon_b} \right)^2 \int_0^d dz' \int_0^d q(z')g(z, z')q(\xi')g(z', \xi') (E_y(\xi') - E_y(z)) d\xi' \quad (13)$$

For the Extended Habashy approximation we begin with the Habashy approximation by writing $E_y(z')$ as $\Gamma(z')E_y^{in}(z')$. When we substitute this into equation (4) we obtain

$$\begin{aligned} E_y(z) &= \Gamma(z)E_y^{in}(z) \\ &\quad - \Gamma^2(z)E_y^{in}(z) \left(\frac{k_b}{2j\epsilon_b} \int_0^d q(z')g(z, z')dz' \right) \\ &\quad + \Gamma(z) \left(\frac{k_b}{2j\epsilon_b} \int_0^d q(z')g(z, z')\Gamma(z')E_y^{in}(z')dz' \right) \end{aligned} \quad (14)$$

This can be manipulated into a more compact form as

$$\begin{aligned} E_y(z) &= \Gamma(z)E_y^{in}(z) [2.0 - \Gamma(z)] \\ &\quad + \frac{k_b}{2j\epsilon_b} \Gamma(z) \int_0^d q(z')g(z, z')\Gamma(z')E_y^{in}(z')dz' \end{aligned} \quad (15)$$

In the final modification applied to the localized approximation, we project both the forward and backward waves onto the scattering coefficient. We model the internal field for an incident plane wave as

$$E_y(z) = \Gamma(z)(Ae^{-jk_b z} + Be^{jk_b z}) \quad (16)$$

where A and B are constants to be determined. The external field then becomes

$$\begin{aligned} 4E_y(z) &= e^{-jk_b z} + \\ &\quad \frac{k_b}{2j\epsilon_b} e^{jk_b z} \int_0^d q(z')\Gamma(z')e^{-jk_b z'} (Ae^{-jk_b z'} + Be^{jk_b z'}) dz' \end{aligned} \quad (17)$$

for $z < z'$. We match the internal and the external fields at the boundary $z = 0$ to compute A and B as

$$A = \frac{\chi_a}{\chi_a(\Gamma(0) - \frac{1}{2}GF(q)) - \frac{1}{2}GF(q)\chi_b} \quad (18)$$

$$B = \frac{\chi_b}{\chi_a(\Gamma(0) - \frac{1}{2}GF(q)) - \frac{1}{2}GF(q)\chi_b} \quad (19)$$

where

$$\chi_a = \Gamma(0) - Q_q(0) + \frac{1}{2}GF(q) \quad (20)$$

$$\chi_b = Q_g(2k_b) - \frac{1}{2}GF(q) \quad (21)$$

$$Q_g(\alpha k_b) = \int_0^d q(z')\Gamma(z')e^{-j\alpha k_b z'} dz' \quad (22)$$

$$G = \Gamma(0)^2 \frac{k_b}{2j\epsilon_b} \quad (23)$$

Here $F(q)$ is the Fourier Transform of q .

2.1 Generalized Local Approximation

We now present a generalization of the local approximation using the Extended Born approximation. We shall show that some of the modifications can be recovered as special cases of this generalization. In the formulation, we adopt the following generic form of the integral equation:

$$E(z) = E_b(z) + \int_0^d \bar{\sigma}(z')G(z, z')E(z')dz' \quad (24)$$

where $G(z, z')$ is the Green function and the support of $\bar{\sigma}(z)$ is $(0, d)$. In this notation, the Green function $G(z, z')$ for the one-dimensional problem is

$$G(z, z') = \frac{k_b}{2j\bar{\sigma}_b} e^{-k_b|z-z'|} \quad (25)$$

The Extended Born approximations are accomplished by repeated iteration of the integral equation, namely,

$$E(z) = \sum_0^{N-1} E_n(z) + e_N(z) \quad (26)$$

where $E_n(z)$ and $e_N(z)$ are

$$E_n(z) = \int_0^d \bar{\sigma}(z')G(z, z')E_{n-1}(z')dz' \quad (27)$$

$$e_N(z) = \int_0^d \bar{\sigma}(z_1)G(z, z_1)dz_1 \int_0^d \bar{\sigma}(z_2)G(z_1, z_2)dz_2 \\ \int_0^d \bar{\sigma}(z_{N-1})G(z_{N-2}, z_{N-1})dz_{N-1} \\ \int_0^d \bar{\sigma}(z_N)G(z_{N-1}, z_N)E(z_N)dz_N \quad (28)$$

with $E_0(z) = E_b(z)$. Only the first $N - 1$ terms in the summation are kept with $e_N(z)$ defining the residual error. $e_N(z)$, the residual error, can alternately be expressed as

$$e_n(z) = \int_0^d \bar{\sigma}(z')G(z, z')e_{n-1}(z')dz' \quad (29)$$

with $e_0(z) = E(z)$. We may apply the localized approximation to equation (28) or equation (29) to derive two different results as follows:

2.2 First Approximation

We apply the localized approximation repeatedly to equation (28) such that

$$E(z_N) \approx E(z_{N-1}) \approx s \approx E(z_2) \approx E(z_1) \approx E(z) \quad (30)$$

and we obtain

$$e_N(z) = \Lambda_N(z)E(z) \quad (31)$$

where $\Lambda_N(z)$ is the N-tuple integral given by

$$\Lambda_N = \int_0^d \bar{\sigma}(z_1)G(z, z_1)dz_1 \int_0^d \bar{\sigma}(z_2)G(z_1, z_2)dz_2 s \\ \int_0^d \bar{\sigma}(z_{N-1})G(z_{N-2}, z_{N-1})dz_{N-1} \\ \int_0^d \bar{\sigma}(z_N)G(z_{N-1}, z_N)dz_N \quad (32)$$

Substituting equation (31) into equation (26), we get for the internal electric field

$$E^{int}(z) \approx \Gamma_N(z) \sum_0^{N-1} E_n(z) \quad (33)$$

where

$$\Gamma_N(z) = [1 - \Lambda_N(z)]^{-1} \quad (34)$$

For $N = 1$ we recover the Habashy approximation and for $N = 2$ we recover the Adopley approximation.

2.3 Second Approximation

We can effect the localized approximation on equation (29) as

$$e_n(z) \approx \Omega(z)e_{n-1}(z) \quad (35)$$

where

$$\Omega(z) = \int_0^d \bar{\sigma}(z')G(z, z')dz' \quad (36)$$

The residual error $e_N(z)$ becomes

$$e_N(z) \approx [\Omega(z)]^N E(z) \quad (37)$$

The internal electric field is then easily shown to be

$$E^{int}(z) \approx \Gamma_N(z) \sum_0^{N-1} E_n(z) \quad (38)$$

where

$$\Gamma_N(z) = [1 - [\Omega(z)]^N]^{-1} \quad (39)$$

Once again we recover the Habashy approximation for $N = 1$. However we do not recover the Adopley approximation when $N = 2$.

We shall investigate and evaluate the effectiveness of the localized approximation (and modifications) in improving and/or enhancing accurate simulation of the total internal electric field. The only setback is that the degree of nonlinearity for the inverse problem as a function of the slab permittivity profile also increases. The feasibility of any particular approximation will then weigh heavily on our ability to

devise an efficient method that can extract the slab profile without disproportionate increase in computation cost. In the inversion studies, we employ Occam's inversion technique [37].

We shall also make comparisons with the Trantanella method which we have extended to include the case of complex conductivity. Briefly in the Trantanella method [19, 21], the internal electric field assumes the form

$$E_y(z') = Ae^{-jk_b z'} + B \frac{k_b}{2j\epsilon_b} \int_0^d q(\xi) e^{-jk_b \xi} e^{-jk_b |z' - \xi|} d\xi \quad (40)$$

where A and B are constants determined from the continuity of the tangential fields at the boundary $z = 0$. The constants A and B are readily evaluated to obtain for $z < 0$ [19, 21]

$$E_y(z) = e^{-jk_b z} + \frac{k_b}{2j\epsilon_b} e^{jk_b z} \frac{Q^2(2k_b)}{Q(2k_b) \left(1 - \frac{k_b d}{2j\epsilon_b} qav\right) - \chi} \quad (41)$$

where

$$\begin{aligned} \chi &= \frac{k_b d}{2\epsilon_b} qav^2 e^{jk_b d} \left(\cos(k_b d) - \frac{\sin(k_b d)}{k_b d} \right), \\ Q(2k_b) &\equiv \int_0^d q(\xi) e^{-2jk_b \xi} d\xi, \\ qav &\equiv \int_0^d q(z) dz. \end{aligned}$$

The major approximation in the Trantanella formulation is assuming the same propagation constant for the slab and background media. Before we embark on any full scale inversion scheme we first reformulate the slab problem in terms of complex conductivity (σ) given by $\bar{\sigma} = \sigma + j\epsilon\omega\epsilon_o$. From the expression derived earlier for the integral equation we can readily show that

$$E_y(z) = E_y^{in}(z) + \frac{k_b}{2j\bar{\sigma}_b} \int_0^d \bar{\sigma}(z') g(z, z') E_y(z') dz' \quad (42)$$

Here $\bar{\sigma}(z) = \bar{\sigma}_s(z) - \bar{\sigma}_b$ and the subscripts s and b refer to slab and background respectively.

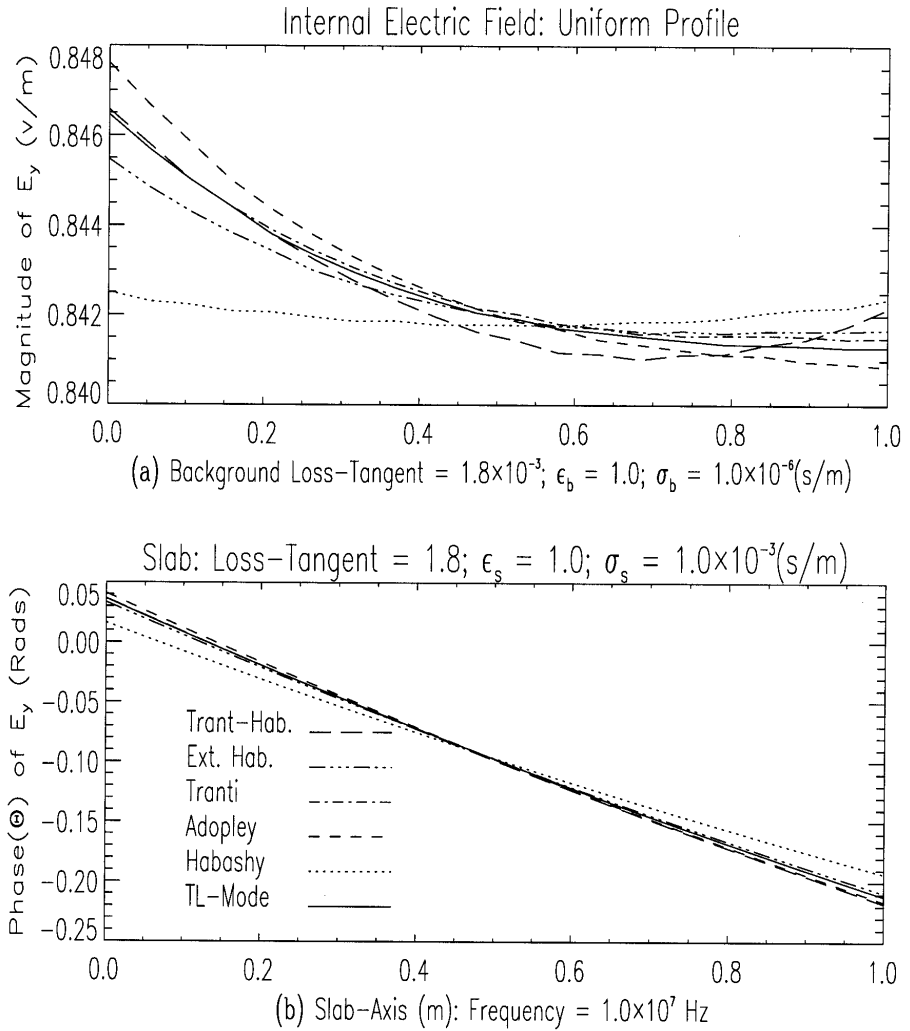


Figure 2. Magnitude and phase plots of internal electric field.

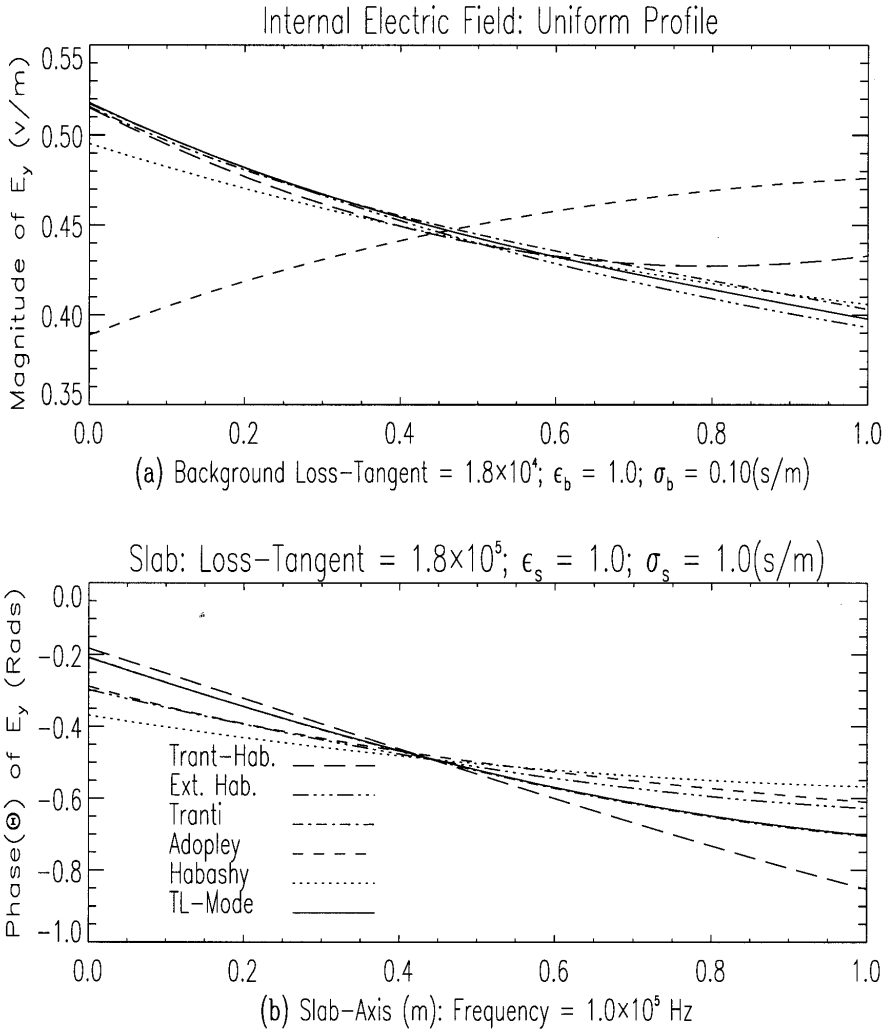
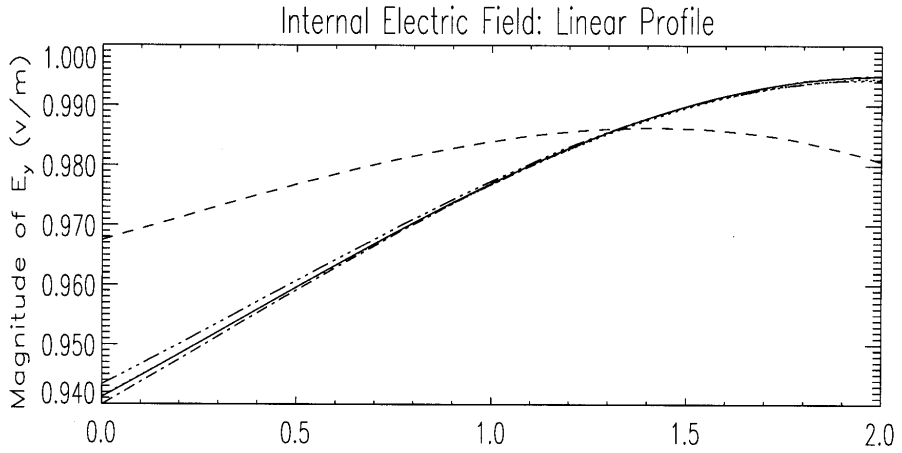
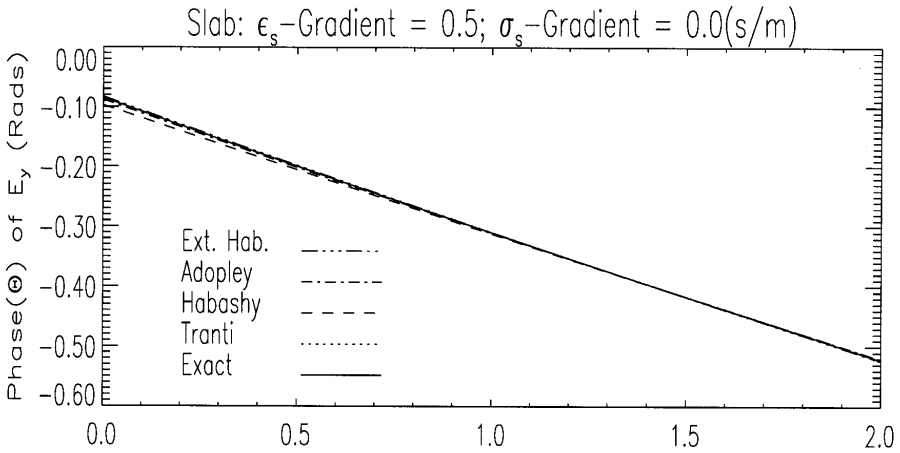


Figure 3. Effect of background and slab loss-tangents on electric field accuracies.



(a) Background Loss-Tangent = 0.0; $\epsilon_b = 1.0$; $\sigma_b = 0.0$ (s/m)



(b) Slab-Axis(m): Frequency = 1.0×10^7 Hz

Figure 4. Effect of relative magnitude of loss-tangents on electric field accuracies.

3. NUMERICAL RESULTS

We present some numerical simulations of the total internal electric field for the piecewise constant and linear complex permittivity or conductivity profiles. These are compared against exact simulation results from transmission-line theory. Each individual model has been tested extensively to evaluate the influence of conduction and displacement currents.

Figures 2 and 3 show the internal electric field simulations of the models against the exact internal field for the constant profile. In Figure 2, the parameters are selected to obtain a loss-tangent of 1.8 for the slab and 1.8×10^{-3} for the homogeneous background medium. The dielectric constant of both the homogeneous background medium and the slab is 1.0. We note that the Habashy model provides the least accurate results. The Trantanella model gives the best result, with perfect match at $z = 0$. We note also that the Extended Habashy model gives much better results than the Habashy model. In Figure 3 we increase the background conductivity to $0.10s/m$ and that of the slab to $1.0s/m$. The Adopley model yields very poor results in the magnitude plots. However, the phase information from the Adopley model is competitive with the other models. We observe good results for the Extended Habashy and the Trantanella models. Figure 4 shows the internal field simulation of models against the exact field for lossless dielectric slab of linear profile. We set $\epsilon - \text{slope}$ at $0.5/m$. All approximations except the Habashy model predict the internal electric field very accurately both in magnitude and phase.

4. INVERSION ALGORITHM

We adopt the Occam's inversion [37] procedure which is based on the notion that any model implemented should be as simple or as smooth as possible. This particular inversion method provides the smoothest model possible within a predefined acceptable data misfit. As measured data is inevitably contaminated with noise, it is unrealistic and in fact undesirable to demand a perfect fit. Indeed seeking a perfect match for measured data introduces phantom structures into the model.

We now present a formal derivation of the model. We define the following quantities:

\mathbf{m}	model parameter vector of length	N
$F[\mathbf{m}]$	the forward model	
\mathbf{d}	observed data vector of length	M
$R_1 = \int (d\mathbf{m}/dz)^2$		
$R_2 = \int (d^2\mathbf{m}/dz^2)^2$		
ν_j	estimated error associated with datum	\mathbf{d}_j

We predict the measured data through a discrete model as $\mathbf{d}_j = F_j[\mathbf{m}]$ and define the acceptability of the model prediction to the actual values with a weighted *Least-square* error

$$\mathcal{X}^2 = \sum_{j=1}^M \left(\frac{\mathbf{d}_j - F_j[\mathbf{m}]}{\nu_j} \right)^2 \quad (43)$$

where as defined earlier ν_j is the uncertainty in the j^{th} datum. The mathematical problem is then, presented with a set of data \mathbf{d}_j with associated uncertainties ν_j , find a model \mathbf{m}_1 that minimizes R_1 or R_2 while \mathcal{X}^2 is kept below some predefined threshold value. This is a nonlinear optimization problem and there is no guarantee that some \mathbf{m}_i will reduce \mathcal{X}^2 to a low enough value. However, we assume that with some constraints on the model parameters consistent with the physics of the problem, we can obtain a good enough model that will provide a reasonable fit to the observed data.

From constraint theory, we apply the Lagrangian multiplier to define our cost function U as

$$U = \|\underline{\delta}\mathbf{m}\|^2 + \mu^{-1} \{ \|\underline{W}\mathbf{d} - \underline{W}F[\mathbf{m}]\|^2 - \chi_*^2 \} \quad (44)$$

where the first term of U is the discrete form of the roughness and the second term is the misfit weighted by the Lagrangian multiplier. \underline{W} is $M \times M$ diagonal matrix $\underline{W} = \text{diag}\{1/\nu_1, 1/\nu_2, \dots, 1/\nu_M\}$. The uncertainties ν_j are assumed to be zero-mean independent Gaussian processes. Thus \mathcal{X}^2 has a χ^2 distribution with expected value of M . In nonlinear analysis we compute $F[\mathbf{m}]$ to the first order due to a perturbation of the model \mathbf{m}

$$F[\mathbf{m}_0 + \Delta] = F[\mathbf{m}_0] + \underline{J}_0\Delta + \varepsilon \quad (45)$$

where ε is a vector with magnitude of $o\|\Delta\|$ and \underline{J}_0 is the Jacobian defined by $\underline{J}_0 = \nabla_{\mathbf{m}}F[\mathbf{m}_0]$ and $\Delta = \mathbf{m} - \mathbf{m}_0$. The implicit assumption is that $F[\mathbf{m}_0]$ is differentiable about the base model \mathbf{m}_0 . If we approximate $F[\mathbf{m}_1]$ by $F[\mathbf{m}_0] + \underline{J}_0\Delta_1$ and define \mathbf{m}_1 as the model that minimizes U , then we obtain from linear theory

$$[\mu\underline{\delta}^T\underline{\delta} + \underline{W}\underline{J}_0)^T(\underline{W}\underline{J}_0)] \mathbf{m}_1 = (\underline{W}\underline{J}_0)^T(\underline{W}\hat{\mathbf{d}})$$

where $\hat{\mathbf{d}} = \underline{W}(\mathbf{d} - F[\mathbf{m}_0] + \underline{J}_0\mathbf{m}_0)$. We then generate an iterative scheme by selecting μ to yield the desired misfit from computation. \mathbf{m}_1 is then used to compute \mathbf{m}_2 until the scheme converges, if at all. It may be shown that if the system converges, it solves the original minimization problem with the final solution independent of the starting values, provided the minimum is unique. However in the present work we have adopted a modified iterative scheme [37, 20] which is as follows: Suppose we have the k^{th} iterate; then we define the vector

$$\mathbf{m}_{k+1}(\mu) = [\mu\underline{\delta}^T\underline{\delta} + \underline{W}\underline{J}_k)^T(\underline{W}\underline{J}_k)]^{-1} (\underline{W}\underline{J}_k)^T(\underline{W}\hat{d}_k)$$

Next a 1-D line search is employed to find μ that minimizes the true misfit given by

$$\mathcal{X}_{k+1}(\mu) = \|\underline{W}\mathbf{d} - \underline{W}F[\mathbf{m}_{k+1}(\mu)]\|$$

This is because any initial guess is usually far from the true model and whatever value of μ selected, \mathcal{X}_k is always greater than χ_* . After a number of minimizations μ is selected for \mathcal{X}_k to match χ_* exactly. We present below some results of our numerical inversion studies using the above inversion algorithm.

4.1 Numerical Inversion Studies

We next present some results from extensive numerical inversions performed using the formulation developed in Section 4. The points $z = 0$ and $z = d$ are referred to as the *measurement boundaries*. Also the actual space occupied by the slab profile within the measurement boundaries we refer to as the *slab region*. All inversion results presented for the constant profile are for a *slab region* of size $d/2$, symmetrically located between the measurement boundaries. This is because we consider this particular profile arrangement, which we term ‘‘inclusion’’ profile, as a realistic approximation to some practical situations.

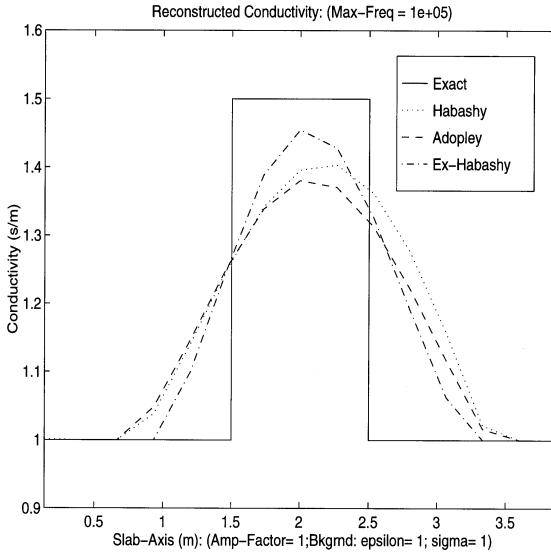


Figure 5. Relative performance of models in “Inclusion” profile reconstruction.

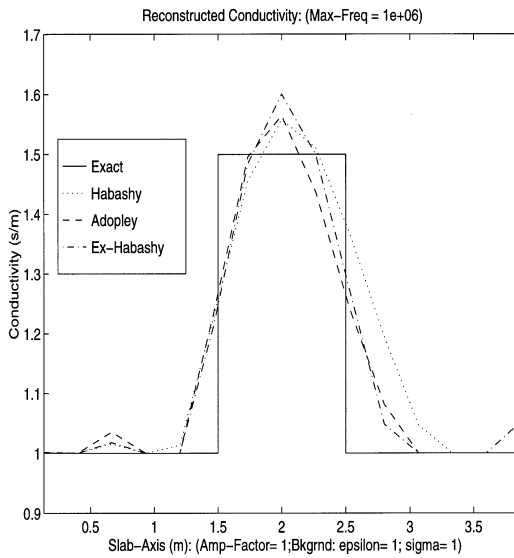


Figure 6. Frequency effect on “Inclusion” profile reconstruction.

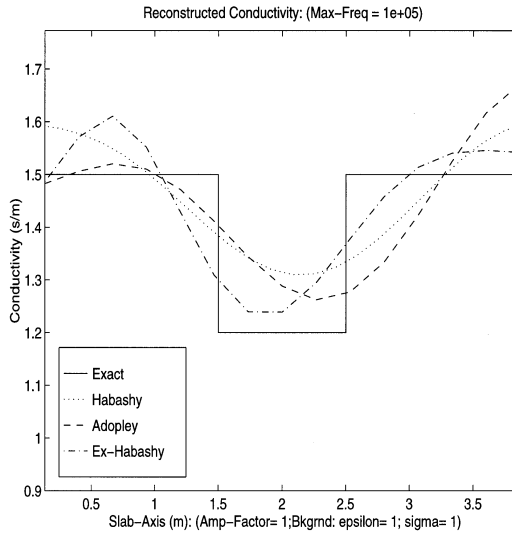


Figure 7. Inverse profile reconstruction.

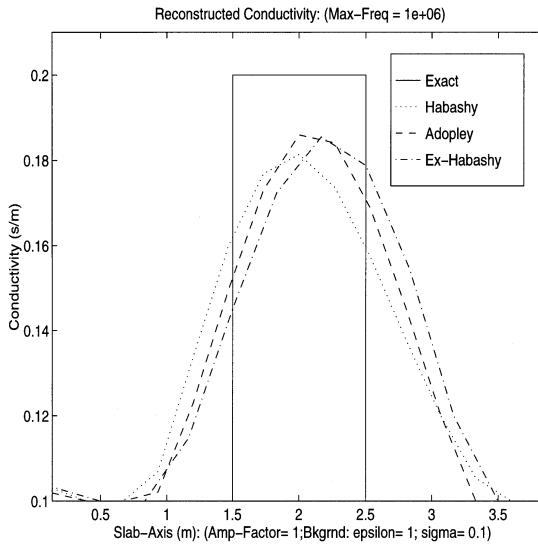


Figure 8. Background complex conductivity effects on profile reconstruction.

In all of our inversion experiments, we employ the scattered electric field at the measurement boundary $z = 0$, which is equivalent to the reflection coefficient. For the piecewise constant profile we generate the synthetic measured data using the transmission-line formulation. The data is then contaminated with Gaussian white-noise of zero mean and 5% standard deviation. This is used for all of our inversions. Data is sampled at frequencies distributed logarithmically between a minimum frequency of $10.0Hz$ and a maximum frequency f_m which is selected individually for each inversion. We select the maximum frequency based on the maximum frequency at which the models accurately simulate the noiseless data.

Figures 5 and 6 portray the relative performances of the different approximation models. In Figures 5 and 6, the maximum frequency of reconstruction is $0.10MHz$ and $1.0MHz$ respectively. At the lower frequency, the Extended-Habashy model predicts the best results. We observe also that the Habashy model produces slightly better results than the Adopley model. However, for reconstruction at the higher frequency shown in Figure 6, the Adopley model produces the overall best results. One should observe in these two figures that the resolution of the profile reconstruction is sharper at the higher frequency. This is found to be generally true. Hence, reconstructions should be done at the highest frequency for which convergence is possible. We also note that, at the higher frequency, the Habashy model yields the least resolution for the reconstructed profile. The Habashy model tends to give higher reconstructed values at the higher frequency.

In Figure 7 the “inclusion” is reversed to produce a depression in the conductivity profile. The three models indicate the conductivity depression quite accurately. However we observed some distinct differences in each model performance. The Adopley model predicts the conductivity profile at the slab leading edge better than the Habashy and the Extended-Habashy models. However, at the slab trailing edge, the Habashy and the Extended Habashy predict better results. The Extended-Habashy predicts the σ depression with a little shift to the left while the Adopley and the Habashy predict with a little shift to the right. In Figure 8 we investigate the effect of background conductivity on model performance. The three models predict roughly the same results. The Habashy model predicts a peak value a little less than the other models. However we also observe that all the models predict peak values less than the actual peak values at the maximum

frequency of $1.0MHz$ employed in the investigation.

5. CONCLUSION

The integral equation that describes the one-dimensional electromagnetic wave propagation is deceptively very simple. The “hidden” difficulty occurs because the elements in the integrand of the integral equation are nonlinearly interdependent. Specifically, the total internal field is a function of the difference between the scatterer and background complex conductivity profiles. The localized approximation as was originally proposed has been extended herein and performances evaluated.

We note from our numerical simulations that, for low contrast between the background and slab complex conductivities, all the approximations give excellent results. Generally, for very low-loss systems the Adopley approximation provides the best results. When the system becomes very lossy the Habashy and the Extended Habashy provide the best results, with a slight edge on accuracy with the Extended Habashy model if numerical noise is negligible. The Trantanella approximation provides very good results at the incident edge of the slab. This we attribute to the formulation. We note that using more terms in the Generalized localized approximation does not guarantee better accuracy. In fact using more than one term can only be justified for very low-loss systems. For high-loss systems the original Habashy approximation provides the best results. Generally, all approximations perform well at moderate frequencies of simulations. However we note deterioration in accuracies at very high frequencies. We also find that the maximum frequency of accurate field simulation increases with decrease in conductivity contrast.

We have presented some reconstruction results using (Occam’s) inversion algorithm on contaminated synthetic data generated from transmission-line theory. The reconstructions are promising. We note, however, that we could not reconstruct very sharp contrasts in conductivity profiles exactly. This is because Occam’s inversion method is L_2 norm dependent. In general for very low-loss profiles the Adopley model gives the best reconstruction. For high contrast in profile conductivities between the homogeneous background and the slab, the best reconstructions are from the Habashy and the extended Habashy models. We note that the Adopley model diverges when the conductivity contrast becomes too large. Also, we observe that the contrast level

for accurate reconstruction for the Adopley model decreases with increase in background conductivity. Concerning speed of performance, the Habashy model is the fastest. We note that the Extended Habashy model becomes very slow when the number of unknowns exceeds 20. This we attribute to the numerical computation of the internal field. The Adopley model performs at moderate speed, but slower than Habashy.

ACKNOWLEDGMENT

Portions of this paper are contained in a dissertation by one of the authors (J.A.K.A), presented in partial satisfaction of the Ph.D. requirements at the University of Arizona. The authors thank Schlumberger-Doll Research for their support of much of this work.

REFERENCES

1. Butler, C., "General analysis of a narrow slot in a conducting screen between half-spaces of different electromagnetic properties," *Radio Sci.*, Vol. 22, No. 7, 1149–1154, 1987.
1. Bleistein, N., and J. K. Cohen, "Nonuniqueness in inverse source problems in acoustics and electromagnetics," *Journal of Mathematical Physics*, Vol. 18, No. 2, 194–201, February 1977.
2. Devaney, A. J., "Nonuniqueness in the inverse scattering problem," *Journal of Mathematical Physics*, Vol. 19, No. 7, 1526–31, July 1978.
3. Devaney, V., and E. Wolf, "Radiating and nonradiating classical currents distributions and the fields they generate," *Physical Review D*, Vol. 8, No. 4, 1044–47, August 1973.
4. Porter, R. P., and A. J. Devaney, "Holography and the inverse source problem," *J. Opt. Soc. Am.*, 72, 327–330, 1982.
5. Stone, R., "A review and examination of results on uniqueness in inverse problems," *Radio Science*, Vol. 22, No. 6, 1026–1030, November 1987.
6. Parker, R. L., "Understanding inverse theory," *Ann. Rev. Earth Planet. Sci.*, 5, 35–64, 1977.
7. Backus, G. E., and J. F. Gilbert, "Numerical application of a formalism for geophysical inverse problems," *Geophys. J. Astron. Soc.*, Vol. 13, 247–276, 1967.
8. Backus, G., and F. Gilbert, "The resolving power of gross Earth data," *Geophys. J. Astron. Soc.*, Vol. 16, 169–205, 1968.

9. Backus, G., and F. Gilbert, "Uniqueness in the inversion of inaccurate gross Earth data," *Phil. Trans. R. Soc. London. Ser. A*, Vol. 266, 123–192, March 1970.
10. Habashy, T. M., E. Y. Chow, and D. G. Dudley "Profile inversion using the renormalized source-type integral equation approach," *IEEE Transactions on Antenna and Propagation*, Vol. 38, 668–682, 1990.
11. Habashy, T. M., R. W. Groom, and B. R. Spies, "Beyond the Born and Rytov approximations: A nonlinear approach to electromagnetic scattering," *Journal of Geophysical Research*, Vol. 98, No. B2, 1759–1775, February 1993.
12. Born, M., and E. Wolf, *Principles of Optics*, Pergamon, New York, 1980.
13. Rytov, S. M., "Diffraction of light by ultrasonic waves," *Izv. Akad. Nauk. SSSR.*, Ser. Fiz. 2, 223, 1937.
14. Oristaglio, M. L., "Accuracy of the Born and Rytov approximations for the reflection and refraction at a plane interface," *Optical Society of America*, Vol. 2, No. 11, 1987–1992, November 1985.
15. Rabiner, L. R., and R. W. Schafer, *Digital Processing of Speech Signals*, Prentice-Hall, Englewood Cliffs, N.J., 1978.
16. Keller, J. B., "Accuracy and validity of the Born and Rytov approximations," *J. Opt. Soc. Am.*, Vol. 59, 1003–1004, August 1969.
17. Sancer, M., and A. D. Varvatsis, "A comparison of the Born and Rytov methods," *Proceedings of the IEEE*, 140–141, January 1970.
18. Torres-Verdin, C., and T. M. Habashy, "Rapid 2.5-dimensional forward modeling and inversion via a new nonlinear scattering approximation," *Radio Science*, Vol. 29, No. 4, 1051–1079, July-August 1994.
19. Trantanella, C. J., "Beyond the Born approximation in one- and two-dimensional profile reconstruction," Ph.D. dissertation submitted to the faculty of the Department of Electrical and Computer Engineering, University of Arizona, May 1994.
20. Adopley, J. A. K., "A comparison among localized approximations in one-dimensional profile reconstruction," Ph.D. dissertation submitted to the faculty of the Department of Electrical and Computer Engineering, University of Arizona, December 1996.
21. Trantanella, C. J., D. G. Dudley and K. A. Nabulsi, "Beyond the Born approximation in one-dimensional profile reconstruction," *J. Opt. Soc. Am.*, Vol. 12, No. 7, 1469–1478, July 1995.

22. Ramo, S., J. R. Whinnery, and T. Van Duzer, *Fields and Waves in Communication Electronics*, Second Edition, John Wiley & Sons Inc., 1984.
23. Tabbara, W., "Reconstruction of Permittivity profiles from a Spectral Analysis of the reflection Coefficient," *IEEE Transactions on Antenna and Propagation*, Vol. AP-27, No. 2, 241–244, March 1979.
24. Chipman, J. S., "On least squares with insufficient observation," *American Statistical Association Journal*, 1078–1111, December 1964.
25. Zhou Y., and C. K. Rushforth, "Least-squares reconstruction of spatially limited objects using smoothness and non-negativity constraints," *Applied Optics*, Vol. 21, No. 7, 1249–1252, April 1982.
26. Tijhuis, A. G., and C. Van Der Worm, "Iterative approach to the frequency-domain solution of the inverse-scattering problem for an inhomogeneous lossless dielectric slab," *IEEE Transactions on Antenna and Propagation*, Vol. AP-32, No. 7, 711–716, July 1984.
27. Kennett, B. L. N., and P. R. Williamson, "Subspace methods for large-scale nonlinear inversion," *Mathematical Geophysics*, 139–154, 1988.
28. Kennett, B. L. N., M. S. Sambridge, and P. R. Williamson, "Subspace methods for large inverse problems with multiple parameter classes," *Geophysical Journal*, 94, 237–247, 1988.
29. Sambridge, M. S., "Non-linear arrival time inversion: constrained velocity anomalies by seeking smooth model in 3-D," *Geophys. J. Int.*, 102, 653–677, 1990.
30. Oldenburg, D. W., and R. G. Eliss, "Inversion of geophysical data using an approximate inverse mapping," *Geophys. J. Int.*, 105, 325–353, 1991.
31. Oldenburg, D. W., P. R. McGillivray, and R. G. Eliss, "Generalized subspace methods for large-scale inverse problems," *Geophys. J. Int.*, 114, 12–20, 1993.
32. Kleinman, R. E., and P. M. van den Berg, "An extended range-modified gradient technique for profile inversion," *Radio Science*, Vol. 28, No. 5, 877–884, 1993.
33. Levenberg, K., "A method for the solution of certain non-linear problems in least squares," *Quart. Appl. Math.*, No. 2, 164–168, July-August 1944.
34. Marquardt, D. W., "Least squares analysis of electron paramagnetic resonance Spectra," *Journal of Molecular Spectroscopy*, 7, 269–279, 1961.

35. Marquardt, D. W., "Generalized inverses, ridge regression, biased linear estimation and nonlinear estimation," *Tecnometrics*, Vol. 2, No. 3, 591–612, 1970.
36. Tikhonov, A. N., and V. Y. Arsenin, *Solutions of Ill-Posed Problems*, V. H. Winston & Sons, Washington, D.C., 1977.
37. Constable, S. C., R. L. Parker, and C. G. Constable, "Occam's inversion: A practical algorithm for generating smooth models from electromagnetic sounding data," *Geophysics*, Vol. 52, No. 3, 289–300, March 1987.
38. Smith, J. T., and J. R. Booker, "Magnetotelluric inversion for minimum structure," *Geophysics*, Vol. 53, No. 12, 1565–1576, December 1988.
39. Rudin, L. I., S. Osher, and E. Fatemi, "Nonlinear total variation based noise removal algorithm," *Physica D*, 60, 259–268 1992.
40. Osher, S., and L. I. Rudin, "Feature-oriented image enhancement using shock filters," *SIAM J. Numer. Anal.*, Vol. 27, No. 4, 919–940, August 1990.
41. van den Berg, P. M., and R. E. Kleinman, "A total variation enhanced modified gradient algorithm for profile reconstruction," *University of Delaware Technical Report*, Newark DE 19716, Vol. 95-4, 1995.
42. Oldenburg, D., "Inversion of electromagnetic data: An overview of new techniques," *Surveys in Geophysics*, 11, 231–270, 1990.
43. Habashy, T. M., and R. Mittra, "On some inversion methods in electromagnetics," *Journal of Electromagnetic Waves and Applications*, Vol. 1, No. 1, 25–58, 1987.
44. Miller, E. L., and A. S. Willsky, "A multiscale, statistically based inversion scheme for linearized inverse scattering problems," *IEEE Transactions on Geoscience and Remote Sensing*, Vol. 34, No. 2, 346–357, March 1996.
45. Zhdanov, M. S., and S. Fang, "Three-dimensional quasi-linear electromagnetic inversion," *Radio Science*, Vol. 31, No. 4, 741–754, July-August 1996.
46. Dudley, D. G., *Mathematical Foundations for Electromagnetic Theory*, IEEE Press, Piscataway, NJ, USA, 1994.
47. Press, W. H., S. A. Teukolsky, W. T. Vetterling, and B. P. Flannery, *Numerical Recipes in Fortran: The Art of Scientific Computing*, Second Edition, Cambridge University Press, 1992.
48. Jeffreys, H., "An alternative to the rejection of observations," *Proceedings of the Royal Society of London*, ser. A, Vol. CXXXVII, 78–87, September 1932.
49. Bender, C. M., and S. A. Orszag, *Advanced Mathematical Methods for Scientists and Engineers*, McGraw-Hill, Inc., 1978.